

## SUPPLEMENTARY MATERIAL

### COMPUTATIONAL DETAILS

Our electronic structure calculations were performed within density functional theory [1, 2] using the all-electron, full potential code WIEN2K [3] based on the augmented plane wave plus local orbitals (APW+lo) basis set [4].

All calculations were well converged with respect to all the parameters used. In particular, we used  $R_{MT}K_{max} = 7.0$  (the product of the smallest of the atomic sphere radii  $R_{MT}$  and the plane wave cutoff parameter  $K_{max}$ ), which determines the size of the basis set. The chosen  $R_{MT}$  are 1.95 a.u. for Sc, 1.73 a.u. for N, 1.79 a.u. for Mg and 1.69 a.u. for O. The calculations used a  $43 \times 43 \times 5$   $k$ -mesh for the integrations over the Brillouin zone. For the structural relaxations we have used the Wu-Cohen (WC) version of GGA [5] that gives better lattice parameters for MgO than PBE [6, 7]. The optimized lattice parameters derived within GGA-WC for MgO and ScN are 4.23 and 4.50 Å, respectively.

An accurate *ab initio* description requires a method able to reproduce the band gap of the individual components as well as their band alignment at the interface, both of which are generally beyond the capabilities of the generalized gradient approximation (GGA) or local density approximation (LDA). To be able to reproduce the bulk gap of ScN, we have used the semilocal potential developed by Tran and Blaha based on a modification of the Becke-Johnson potential (TB-mBJ) [8, 9]. This is a local approximation (local in the density and the kinetic energy density) to an atomic exact-exchange potential and a screening term + GGA correlation that allows the calculation of band gaps with an accuracy similar to the much more expensive GW or hybrid methods [8, 9]. The TB-mBJ functional is a potential-only functional, i.e., there is no corresponding TB-mBJ exchange-correlation energy functional. In this respect it is applied as a self-energy correction, and one based on improved intra-atomic exchange processes. The bandstructure for bulk ScN obtained within TB-mBJ gives the correct band gap and is shown in the Supplementary Fig. 1.

Based on the agreement with the experiments for ScN bulk, TB-mBJ was the scheme applied to the ScN/MgO (111) multilayers. We have modeled MgO/ScN(111) multilayers which are 2- to 7-ScN layers thick. A barrier of 3-4 MgO layers (about 1 nm thick) between ScN blocks has been used for all the calculations, checking that it is sufficient to guar-

antee the lack of interaction between ScN blocks. The multilayers are modeled with the in-plane lattice parameters constrained to those of MgO (fixed to the value 4.23 Å, obtained by optimizing the cell volume within WC-GGA).

For all the multilayers we performed calculations with fully relaxed atomic positions also optimizing the value of the  $c$ -lattice parameter (off-plane), i.e. allowing atomic displacements along the  $c$ -axis and thus relaxing the inter-plane distances for the structures with different number of ScN layers. The optimized values of the  $c$ -lattice parameter result in a slight increase from the value obtained by constructing the multilayers from the MgO bulk unit cell, of about 1% to 2% for multilayers two to seven ScN layers thick. This is expected, as the in-plane lattice parameter inside the ScN blocks is constrained to that of MgO, which is smaller (4.23 Å versus 4.50 Å for the cubic phase of ScN). The ScN block is subjected to compressive strain due to the lattice mismatch (of about 5%, an amount that can be sustained for several layers).

One of the main features in the calculated relaxed geometry is the presence of a considerable polar distortion in the ScN layers while there is negligible distortion on the MgO side. The atomic displacements are exclusively along the  $c$ -axis resulting on one shorter (2.07-2.09 Å) and one longer (2.15-2.23 Å) Sc-N or Sc-O bond as can be seen in Fig. 1.

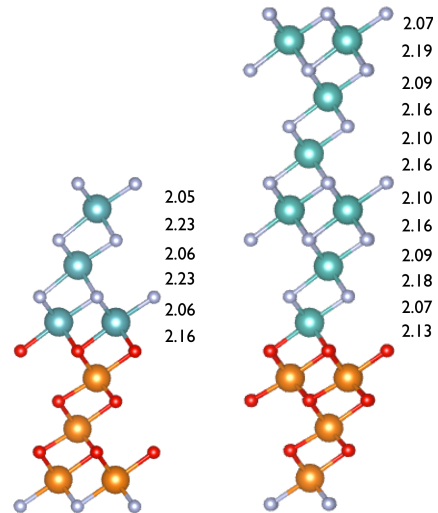


FIG. 1: **Relaxed structure of MgO/ScN (111) multilayers** Unit cell of the the relaxed 3- and 6- ScN layers thick with Sc atoms in blue, N atoms in gray. Mg atoms in orange and O atoms in red. The average distances between layers along the  $z$  axis (in Å) are shown.

The transport properties were calculated using

a semiclassical solution based on Bloch-Boltzmann transport theory within the constant scattering time approximation by means of the BoltzTraP code [10], which uses the energy eigenvalues calculated by the WIEN2K code. The constant scattering time approximation assumes that the energy dependence of the scattering time at a given temperature and doping level is negligible on the scale of  $k_B T$ . In this case, denser k-meshes are required, in our case up to  $118 \times 118 \times 14$  to reach convergence.

## ELECTRONIC STRUCTURE OF BULK SCN

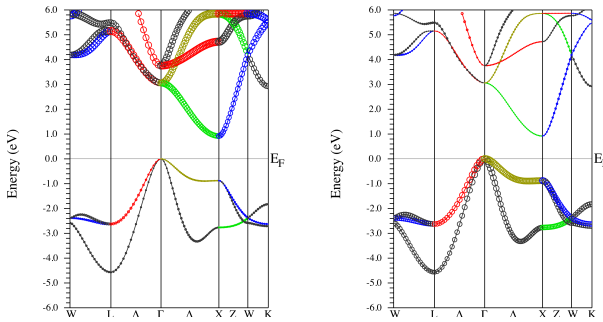


FIG. 2: **Electronic structure of bulk ScN** Band structure with orbital character shown by circle size, for ScN using the TB-mBJ potential. Left panel: Sc 3d; right panel: N 2p.

Early density functional theory-based calculations employing the LDA [11] or  $X\alpha$ [12, 13] approximations predicted ScN to be a semimetal. In order to overcome the well-known underestimation of the LDA band gap, more advanced exact exchange and screened exchange calculations have been performed and showed that ScN is a semiconductor with an indirect  $\Gamma$ -X band gap, consistent with experiments. However, the calculated band gap of 1.6 eV is significantly larger than the experimental value of 0.9 eV [14]. LDA/GGA-PBE/GGA-WC+ $U$ [15] calculations using a  $U$  value as high as 6 eV are only able to open an indirect gap of 0.40 to 0.55 eV, respectively, far from the one determined experimentally [16]. LDA calculations complemented with estimated quasiparticle corrections and calculations of the optical response give an indirect band gap of 0.9 eV with a first direct gap at X of 2 eV. [17]  $G_0W_0$  quasiparticle calculations predict ScN to have an indirect band gap between  $\Gamma$ -X of 0.99 eV [18]. Also hybrid functionals show the opening of a band gap of 0.9 eV [19].

Figure 2 shows the band structure with band character plot (N and Sc character highlighted) for ScN

obtained within TB-mBJ. Taking the usual valence for N, the average valence for the Sc cations is +3 ( $d^0$ ). The band gap is formed between occupied N-2p and unoccupied Sc-3d states and the experimental value of the gap is reproduced: an indirect band gap of 1.0 eV between  $\Gamma$ -X is obtained as well as the direct gap of 2.1 eV at X.

## ELECTRONIC STRUCTURE OF MgO/SCN(111) MULTILAYERS

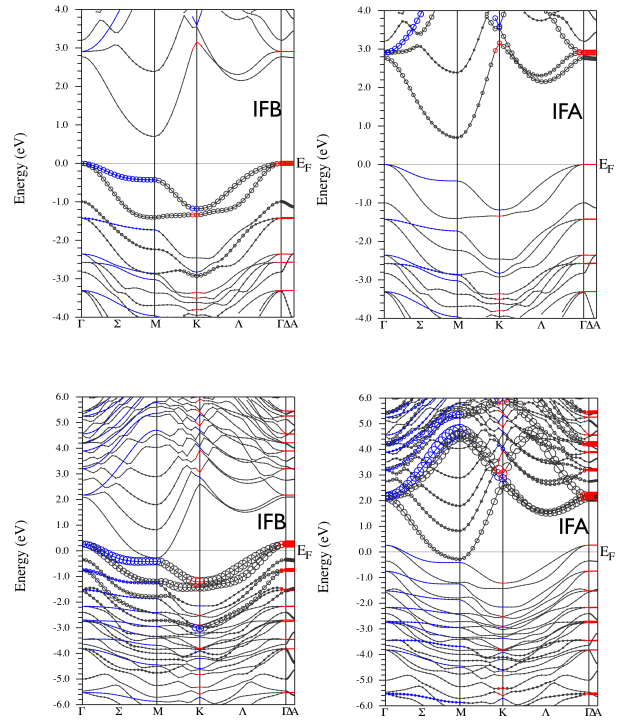


FIG. 3: **Bandstructure with band character plot for MgO/ScN (111) multilayers.** Sc-d atom at IFA(right) and N-p levels at IFB (left) for ScN/MgO(111) multilayers three (top panel) and six (bottom panel) ScN-layers-thick.

Figure 3 shows the band structures with band character plot that complement Fig. 3 in the main text that shows only the DOS. The bands crossing the Fermi level are indeed N-p at IFB and Sc-d at the IFA.

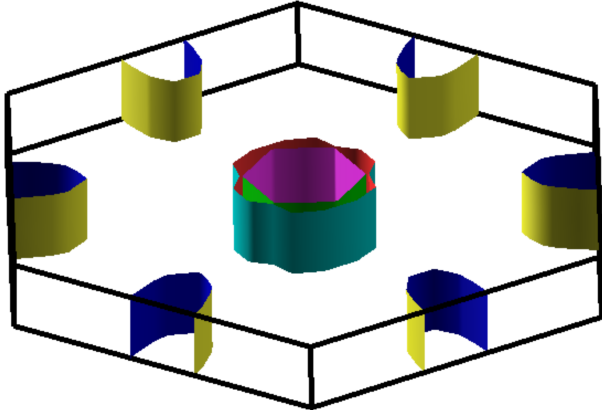


FIG. 4: Fermi surface plots for hole and electron pockets obtained for ScN/MgO(111) multilayers 6 ScN layers thick the nearly circular hole pocket is centered at  $\Gamma$  whereas the nearly circular electron pocket is centered at the hexagonal zone face ( $M$  point).

Fig. 4 shows that these bands give rise to the nearly circular Fermi surfaces coming from the electron and hole pockets, as discussed in the main text.

---

[1] P. Hohenberg and W. Kohn, Phys. Rev. **136**, B864 (1964).  
 [2] R. O. Jones and O. Gunnarsson, Rev. Mod. Phys. **61**, 689 (1989).  
 [3] K. Schwarz and P. Blaha, Computational Materials Science **28**, 259 (2003), ISSN 0927-0256, proceed-

ings of the Symposium on Software Development for Process and Materials Design.

[4] E. Sjöstedt, L. Nördstrom, and D. Singh, Solid State Communications **114**, 15 (2000), ISSN 0038-1098.  
 [5] Z. Wu and R. E. Cohen, Phys. Rev. B **73**, 235116 (2006).  
 [6] J. P. Perdew, K. Burke, and M. Ernzerhof, Phys. Rev. Lett. **77**, 3865 (1996).  
 [7] F. Tran, R. Laskowski, P. Blaha, and K. Schwarz, Phys. Rev. B **75**, 115131 (2007).  
 [8] F. Tran and P. Blaha, Phys. Rev. Lett. **102**, 226401 (2009).  
 [9] D. Koller, F. Tran, and P. Blaha, Phys. Rev. B **83**, 195134 (2011).  
 [10] G. K. Madsen and D. J. Singh, Computer Physics Communications **175**, 67 (2006).  
 [11] R. Monnier, J. Rhyner, T. M. Rice, and D. D. Koelling, Phys. Rev. B **31**, 5554 (1985).  
 [12] P. Neckel, R. Rastl, P. Eibler, P. Weinberger, and K. Schwarz, J. Phys. C **9**, 579 (1976).  
 [13] R. Eibler, M. Dorrer, and A. Neckel, Theor. Chim. Acta **63**, 133 (1983).  
 [14] D. Gall, M. Stdele, K. Jirrendahl, I. Petrov, P. Desjardins, R. T. Haasch, T.-Y. Lee, and J. E. Greene, Phys. Rev. B **63**, 125119 (2001).  
 [15] A. Lichtenstein, V. Anisimov, and J. Zaanen, Phys. Rev. B **52**, R5467 (1995).  
 [16] M. Abu-Jafar, A. Abu-Labdeh, and M. El-Hasan, Computational Materials Science **50**, 269 (2010), ISSN 0927-0256.  
 [17] W. R. L. Lambrecht, Phys. Rev. B **62**, 13538 (2000).  
 [18] A. Qteish, P. Rinke, M. Scheffer, and J. Neugebauer, Phys. Rev. B **74**, 245208 (2006).  
 [19] S. Kerdsonpanya, B. Alling, and P. Eklund, Phys. Rev. B **86**, 195140 (2012).